

THE DEEP2 GALAXY REDSHIFT SURVEY: MEAN AGES AND METALLICITIES OF RED FIELD GALAXIES AT $z \sim 0.9$ FROM STACKED KECK DEIMOS SPECTRA¹

RICARDO P. SCHIAVON,² S. M. FABER,³ NICHOLAS KONIDARIS,³ GENEVIEVE GRAVES,³
 CHRISTOPHER N. A. WILLMER,^{3,4} BENJAMIN J. WEINER,⁵ ALISON L. COIL,^{4,6,7} MICHAEL C. COOPER,⁶
 MARC DAVIS,⁶ JUSTIN HARKER,³ DAVID C. KOO,³ JEFFREY A. NEWMAN,^{6,7,8} AND RENBIN YAN⁶

Received 2006 February 10; accepted 2006 September 11; published 2006 October 16

ABSTRACT

As part of the DEEP2 galaxy redshift survey, we analyze absorption line strengths in stacked Keck DEIMOS spectra of red field galaxies with weak to no emission lines, at redshifts $0.7 \leq z \leq 1$. Comparison with models of stellar population synthesis shows that red galaxies at $z \sim 0.9$ have mean luminosity-weighted ages of the order of only 1 Gyr and at least solar metallicities. These ages cannot be reconciled with a scenario in which all stars evolved passively after forming at very high z . Rather, a significant fraction of stars can be no more than 1 Gyr old, which means that some star formation in the stacked populations continued to at least $z \sim 1.2$. Furthermore, a comparison of these distant galaxies with a local SDSS sample, using stellar population synthesis models, shows that the drop in the equivalent width of H δ from $z \sim 0.9$ to 0.1 is less than that predicted by passively evolving models. This admits two interpretations: either each individual galaxy experiences continuing low-level star formation, or the red-sequence galaxy population from $z \sim 0.9$ to 0.1 is continually being added to by new galaxies with younger stars.

Subject headings: galaxies: distances and redshifts — galaxies: evolution — galaxies: stellar content

1. INTRODUCTION

The formation of early-type galaxies is one of the ongoing riddles of modern cosmology. According to the leading models, massive early-type galaxies have been assembled hierarchically from the merging of less massive structures. Because such mergers are seen locally to be accompanied by star formation (e.g., Schweizer & Seitzer 1992), one of the best ways to test the hierarchical formation paradigm is by determining the star formation history of early-type galaxies. This can be achieved by estimating the ages of stars in galaxies from their integrated light, through comparison with stellar population synthesis models. Several groups have attempted this from observations of distant massive galaxies (e.g., Le Borgne et al. 2006; Treu et al. 2005; Daddi et al. 2005; Longhetti et al. 2005 and references therein). However, spectroscopic dating of stellar populations older than ~ 1 Gyr is best achieved by simultaneously matching the strengths of Balmer and metal lines in their integrated spectra, in order to break the age-metallicity degeneracy. So far, observational difficulties have prevented such detailed studies for all but local samples (e.g., González 1993; Trager et al. 2000; Kuntschner 2000; Caldwell et al. 2003; Eisenstein et al. 2003; Thomas et al. 2005; Schiavon 2006 and references therein).

In this Letter we present the analysis of absorption line strengths measured in stacked integrated Keck DEIMOS spectra of *red galaxies* with redshifts between 0.7 and 1, as part

of the DEEP2 (Deep Extragalactic Evolutionary Probe 2) survey (Davis et al. 2003). We find that these galaxies have mean light-weighted single stellar population (SSP) ages of the order of only 1 Gyr and metallicities at least solar. Since these objects are observed several billion years after the big bang, this result suggests that stars populating these galaxies were formed during an extended period of time.

2. SAMPLE AND DATA

The data used in this Letter consist of k -corrected U and B absolute magnitudes in the Vega system and 1 hr exposure Keck DEIMOS (Deep Imaging Multi-Object Spectrograph; Faber et al. 2003) spectra from DEEP2 (Davis et al. 2003). Redshift determinations are described in Davis et al. (2003), and rest-frame M_B magnitudes and $U - B$ colors were derived from Canada-France-Hawaii Telescope (CFHT) BRI photometry and redshifts by Willmer et al. (2006). The signal-to-noise ratio (S/N) of each 1 hr exposure spectrum is not high enough for accurate measurement of absorption line indices, so we stack spectra of hundreds of galaxies, selected in bins of color, luminosity, and redshift.

2.1. Sample Selection

Our goal is to study the evolution of red-sequence galaxies, so we first select galaxies by color, as illustrated in the left panel of Figure 1, where data for 17,745 DEEP2 galaxies with $0.7 \leq z \leq 1.05$ were used to produce a contour plot in rest-frame color-magnitude space. Red-sequence galaxies (RSGs) are chosen to be those with $U - B \geq 0.25$, making up a total of 1941 objects. Ideally, we would also like to select galaxies on the basis of morphology, but we lack that information for this sample. In order to minimize contamination by reddened late-type galaxies (LTGs), we impose another cut, based on the equivalent width (EW) of [O II] $\lambda 3727$ (as defined by Fisher et al. 1998). This is illustrated in the right panel of Figure 1, where a histogram of [O II] EWs is shown for all RSGs in our sample. The distribution is strongly peaked at very low [O II]

¹ Based on observations taken at the W. M. Keck Observatory.

² Department of Astronomy, University of Virginia, P.O. Box 3818, Charlottesville, VA 22903-0818.

³ UCO/Lick Observatory and Department of Astronomy and Astrophysics, University of California, Santa Cruz, CA 95064.

⁴ Steward Observatory, University of Arizona, Tucson, AZ 85721.

⁵ Department of Astronomy, University of Maryland, College Park, MD 20742-2421.

⁶ Department of Astronomy, University of California, Berkeley, 601 Campbell Hall, Berkeley, CA 94720-3411.

⁷ Hubble Fellow.

⁸ Lawrence Berkeley National Laboratory, Berkeley, CA 94720.

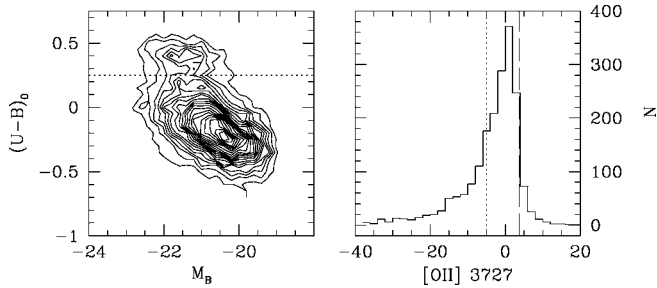


FIG. 1.—*Left*: Rest-frame color-magnitude diagram of 17,745 DEEP2 galaxies. Our sample of RSGs is defined by $U - B > 0.25$ (objects above the dotted line). *Right*: Histogram of $[\text{O II}] \lambda 3727$ EWs for RSGs. Because the $[\text{O II}]$ line is superposed on strong absorption lines, $\text{EW} = 0$ is not achieved for zero emission. Instead, no $[\text{O II}]$ emission happens when $\text{EW}([\text{O II}]) = 3.7 \text{ \AA}$ (dashed line; N. Konidaris et al. 2006, in preparation), with emission-line galaxies having lower EWs. All galaxies with $\text{EW}([\text{O II}]) \leq -5 \text{ \AA}$ (dotted line) are excluded from the sample.

emission, with a long tail toward strong $[\text{O II}]$. Contamination by LTGs is likely to be more important in the strong emission line regime, so we remove from our sample all galaxies with $[\text{O II}] \text{ EW} \leq -5 \text{ \AA}$. It is important to estimate how effectively this emission-line cut cleans our sample of LTG contamination. Weiner et al. (2005) showed that at $z \leq 1$ LTGs comprise roughly 25% of the red-sequence population. Looking at the middle panel of their Figure 16, we estimate that at least $\frac{3}{4}$ of the red LTGs in their study have $[\text{O II}]$ emission stronger than our adopted threshold. Therefore, we estimate that contamination of our sample by LTGs is at most at the 5% level. Our emission-line cut leaves a large number of (presumably morphologically early-type) galaxies in the low emission line regime. We believe that these are mostly active galactic nuclei (AGNs), on the basis of the ratios between $[\text{O II}]$ and residual Balmer line emission (N. Konidaris et al. 2006, in preparation), as found for low-redshift RSGs (Phillips et al. 1986; Rampazzo et al. 2005; Yan et al. 2006).

The color and emission-line cuts leave us with a master sample of 1160 galaxies. We create six somewhat smaller subsamples out of this set of galaxies, three with varying colors but the same redshift range, and three with varying redshifts but consistent colors and luminosities. The color and redshift limits of each bin are listed in Table 1. In order to compare objects with similar stellar masses, galaxies in the color and redshift subsamples were further selected within 1 mag wide M_B intervals in which the central magnitude was chosen to be consistent with passive evolution from the age and metallicity of the high- z sample. However, adopting the same M_B interval

for each z bin does not change the results. The numbers of galaxies in each bin are listed in Table 1.

2.2. Stacked Spectra and Lick Indices

All the galaxy spectra were visually inspected in order to clean the sample of a few misclassified stars, galaxies with wrong redshifts, and zero-S/N spectra. A rough relative fluxing was achieved by dividing each spectrum by the normalized throughput of the DEIMOS spectrograph with the 1200 line mm^{-1} grating. Before co-addition, the spectra were brought to rest frame and then normalized through division by the average (σ clipped) counts within the 3900–4100 \AA interval. Co-addition was performed adopting a σ clipping procedure to eliminate sky-subtraction residuals, zero-count pixels due to CCD gaps, and other spectral blemishes. After several tests the best results were obtained when a single 3σ clipping iteration was adopted. More than 90% of all galaxies in a given bin contribute to the stacked spectrum at any wavelength. No clipping was performed in the region of $[\text{O II}] \lambda 3727$. In Figure 2a we compare one of our stacked spectra with a SSP model from Schiavon (2006). In order to match the overall flux distribution, the observed spectrum was dereddened by $E(B - V) = 0.2$. Since the observations are not properly flux-calibrated, we do not believe that this $E(B - V)$ reflects the average reddening in the sample, and this correction has the sole purpose of bringing observations and theory to a common relative scale, thus highlighting the outstanding agreement between the observed and synthetic spectra.⁹

The $\text{H}\delta_F$ and $\text{Fe}4383$ indices, which are chiefly sensitive to age and $[\text{Fe}/\text{H}]$, respectively, were measured in the stacked spectra. The spectra were first broadened to the Lick resolution as given by Schiavon (2006), and the indices were measured following definitions by Worthey & Ottaviani (1997) and Worthey et al. (1994). Velocity dispersions (σ) were measured in the stacked spectra through Fourier cross-correlation using the IRAF `rv.fxcor` routine. The template adopted was a solar-metallicity, 2 Gyr old SSP model spectrum from Schiavon (2006). Line indices were converted to $\sigma = 0 \text{ km s}^{-1}$ using the corrections by Schiavon (2006) and adopting the σ determined for each stacked spectrum. The latter are listed in Table 1. We do not attempt to convert the line indices to the Lick system, aside from smoothing them to the Lick resolution. However, zero-point differences should be very small, given

⁹ Assuming that $E(B - V) = 0.2$ arises from dust and not from flux calibration errors has no impact on our results, as MacArthur (2005), using a multipopulation model including selective extinction, showed that the indices studied here are only affected by reddening in the presence of strong ongoing star formation.

TABLE 1
DATA FOR GALAXIES USED IN STACKED DEEP2 SPECTRA

Bin	z	Absolute Magnitude ^a	$U - B$	$\text{H}\delta_F$	$\text{Fe}4383$	σ (km s^{-1})	N^b
Low z	[0.7, 0.8]	[−21.57, −20.57]	[0.25, 0.60]	1.8 ± 0.1	3.7 ± 0.5	190	113
Intermediate z	[0.8, 0.9]	[−21.70, −20.70]	[0.25, 0.60]	1.8 ± 0.1	3.0 ± 0.2	170	288
High z	[0.9, 1.0]	[−21.86, −20.86]	[0.25, 0.60]	1.8 ± 0.2	...	180	167
Red	[0.75, 0.95]	[−21.76, −20.76]	[0.45, 0.60]	1.6 ± 0.2	3.7 ± 0.3	190	129
Intermediate	[0.75, 0.95]	[−21.76, −20.76]	[0.35, 0.45]	1.8 ± 0.1	3.2 ± 0.2	170	228
Blue	[0.75, 0.95]	[−21.76, −20.76]	[0.25, 0.35]	2.3 ± 0.2	2.4 ± 0.3	170	119
SDSS Lum 215	0.171	[−22.0, −21.5]	...	0.66 ± 0.01	4.32 ± 0.02	235	5412
SDSS Lum 210	0.143	[−21.5, −21.0]	...	0.82 ± 0.01	4.22 ± 0.02	210	6477

NOTES.—Numbers in brackets correspond to intervals adopted to select galaxies in different bins. Single numbers correspond to measurements taken in stacked spectra or, in the case of $U - B$ for DEEP2 and z for SDSS, average values within a given bin.

^a Absolute magnitudes are M_B for DEEP2 and M_r for SDSS.

^b Number of galaxies in a bin.

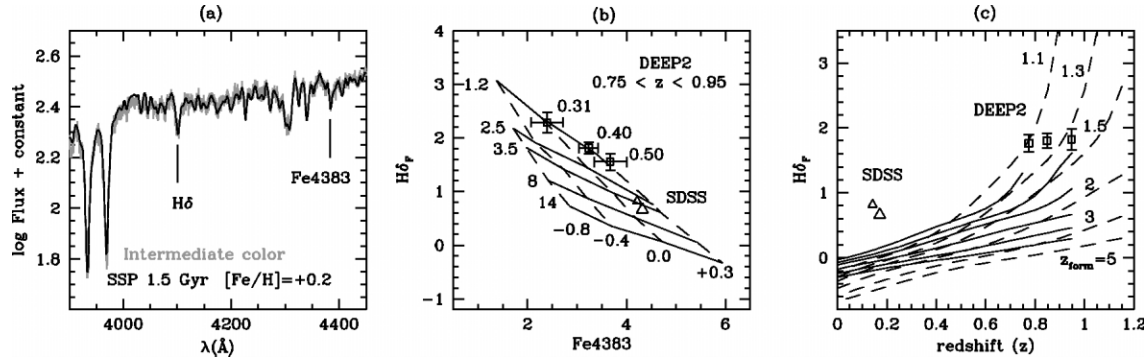


Fig. 2.—(a) Comparison between the stacked spectrum for the intermediate color bin (see Table 1) and that for a model SSP from Schiavon (2006). The two absorption lines studied here are indicated. This plot illustrates the high S/N of the stacked spectra and the high quality of the models, which reproduce all the main absorption lines in the observed spectrum very well. (b) Measurements from RSG stacked spectra vs. predictions of SSP models. Squares with error bars indicate DEEP2 galaxies, and triangles indicate SDSS galaxies from Eisenstein et al. (2003). For SDSS data, symbol size correlates with luminosity. DEEP2 galaxies are binned by color and have absolute magnitudes and redshifts within the intervals indicated in the label and in Table 1. The mean $U - B$ colors of the DEEP2 bins are indicated to the right of each data point. The models are those of Schiavon (2006) for $[\alpha/\text{Fe}] = +0.4$. Same-age and same-metallicity models are connected by solid and dashed lines, respectively. Model age ($[\text{Fe}/\text{H}]$) ranges from 1.2 to 14 Gyr (-0.8 to $+0.3$ dex). The mean SSP ages of DEEP2 galaxies are ~ 1.2 Gyr, regardless of color. They are younger than SDSS galaxies, as expected. Their $[\text{Fe}/\text{H}]$ -values range between solar and $+0.3$. (c) DEEP2 data from the redshift-selected sample compared with SSP models in a redshift vs. $H\delta_F$ plot. Predictions from SSP models with supersolar metallicity and a range of formation redshifts, z_{form} , are shown as solid ($[\text{Fe}/\text{H}] = +0.2$, $[\alpha/\text{Fe}] = 0$) and dashed ($[\text{Fe}/\text{H}] = +0.3$, $[\alpha/\text{Fe}] = +0.4$) lines. DEEP2 galaxies are consistent with z_{form} ranging from 1.1 to 1.3 (1.3 to 1.5 if $[\text{Fe}/\text{H}] = 0$). This indicates that star formation was prolonged in these galaxies. Galaxies at high and low z are *not* connected by lines of passive evolution, which indicates either that star formation continued in these galaxies from $z \sim 0.9$ to ~ 0.15 or that the RSG population is continually being added to by new galaxies with younger stars from $z \sim 0.9$ to the present.

that the Schiavon (2006) models are based on fluxed spectra and the DEEP2 spectra are corrected from instrumental throughput. Finally, Balmer lines were corrected for emission-line infill, which was estimated from $\text{EW}([\text{O II}])$, adopting $\text{EW}([\text{O II}])/\text{EW}(\text{H}\alpha) = 5$ (Yan et al. 2006) and $\text{EW}(\text{H}\delta) = 0.13\text{EW}(\text{H}\alpha)$. The correction to $H\delta_F$ is smaller than 0.2 \AA , corresponding to less than ~ 0.1 Gyr in age.

2.3. Local Sample

Galaxy evolution is best assessed when distant and local samples of similar objects are contrasted using evolutionary models. It is vital that the nearby and distant samples be defined consistently, to ensure that they represent objects of the same class. For a local counterpart to the distant DEEP2 sample we use the Sloan Digital Sky Survey (SDSS) data from Eisenstein et al. (2003), who provide stacked flux-calibrated spectra of RSGs binned by absolute magnitude, environment, and redshift. Because the DEEP2 stacked spectra include galaxies from all environments, we chose to use stacked spectra for a similarly defined sample from Eisenstein et al. (their “All” sample). In order to restrict the comparison to galaxies with similar absolute magnitudes, we exclude both the lowest and highest magnitude bins of the Eisenstein et al. sample from the analysis. Stacked spectra were downloaded from D. Eisenstein’s home page and submitted to the same treatment as described above. Key data for the Eisenstein et al. (2003) sample are listed in Table 1.

3. MEAN AGES AND METALLICITIES

Lick indices measured in the stacked spectra are compared with SSP models in Figure 2b. Shown are indices measured in the Eisenstein et al. (2003) spectra and those from the color-selected DEEP2 subsamples. The models were computed adopting $[\alpha/\text{Fe}] = +0.4$, $[\text{C}/\text{Fe}] = +0.15$, and $[\text{N}/\text{Fe}] = +0.3$ (see Schiavon 2006 for details), but the results are insensitive to the detailed abundance pattern.

The main result of this Letter is contained in Figure 2b. The stellar populations of field RSGs at $z \sim 0.9$ are young, with a mean luminosity-weighted age of only ~ 1.2 Gyr. Adoption of

solar-scaled models would imply only slightly older ages, by roughly 0.5 Gyr. Iron abundances range from $[\text{Fe}/\text{H}] \sim 0$ to $\sim +0.3$. As expected, the stellar populations in the local SDSS galaxies are older than those at $z \sim 0.9$, with mean ages ranging between 3 and 5 Gyr and supersolar $[\text{Fe}/\text{H}]$. The time difference between the characteristic redshifts of the DEEP2 and SDSS samples is over 5 Gyr, so the expected mean ages of SDSS galaxies under passive evolution should be over 6 Gyr. This does not seem to be the case: the mean SDSS galaxy age is only ~ 4 Gyr. We note that the Schiavon (2006) models match the data for Galactic globular clusters and—most importantly—those for the open cluster M67 (3.5 Gyr, $[\text{Fe}/\text{H}] = 0$) to within 1 Gyr in age and 0.1 dex in $[\text{Fe}/\text{H}]$.

Another way of viewing this result is illustrated in Figure 2c, where DEEP2 and SDSS galaxies are compared with passively evolving SSP models in a redshift versus $H\delta_F$ plot. The DEEP2 data plotted here come from the redshift-selected subsample (see Table 1). The lines correspond to model predictions for SSP evolution assuming various redshifts of formation (z_{form}) and adopting a concordance *Wilkinson Microwave Anisotropy Probe* (WMAP) cosmology (Spergel et al. 2003). Figure 2c shows that the data for field RSGs require $z_{\text{form}} \sim 1.1$ – 1.3 , when they are modeled using SSPs with supersolar metallicity. Moreover, the distant and local (SDSS) samples are not connected by lines of passive evolution, which indicates the occurrence of star formation between $z \sim 0.9$ and ~ 0.1 (see also Gebhardt et al. 2003). This could be due either to in situ star formation or to the arrival onto the red sequence of new galaxies coming from the blue cloud after cessation of star formation. Figure 2c also makes clear that these results are valid regardless of the $[\alpha/\text{Fe}]$ ratio of the models adopted (dashed vs. solid lines). The results also relatively insensitive to metallicity: adoption of solar-metallicity models (not shown) would result in slightly higher redshifts of star formation, $z_{\text{form}} \sim 1.3$ – 1.5 .

4. CONCLUSIONS AND CAVEATS

The results presented in this Letter should be interpreted carefully. Ages and metallicities inferred from comparison of

integrated galaxy spectra with SSP models are luminosity-weighted averages, whereas the real stellar populations consist of stars with a range of ages. Therefore, we are not claiming that the stars in the DEEP2 galaxies plotted in Figure 2*b* are uniformly ~ 1.2 Gyr old; many must be considerably older. Likewise, we are not proposing that the average galaxy plotted in Figure 2*c* sprang into existence at $z \sim 1.3$. But the strength of H δ in the stacked integrated spectra of field RSGs indicates that they harbor young and/or intermediate-age stars both locally and at $z \sim 0.9$. Since the universe was roughly 6 Gyr old at $z \sim 0.9$, this result cannot be reconciled with models in which *all* stars in these galaxies were formed at very high redshifts ($z > 3$) and evolved passively ever since. In fact, it appears that star formation in these galaxies was prolonged, as the SDSS data suggest that it must have continued on, at least in small amounts, from $z \sim 0.9$ to 0.1. The fact that we see no evolution in [Fe/H] seems to indicate that the bulk of star formation has occurred before $z \sim 0.9$.

The presence of young/intermediate-age stars in RSGs can be accounted for by at least two scenarios. So-called frosting models (e.g., Trager et al. 2000) include small amounts of recent in situ star formation. On the other hand, “quenching” models (e.g., Bell et al. 2004; Faber et al. 2006) suggest that blue galaxies migrate to the red sequence after cessation of star formation, possibly associated with a merger event and/or enhanced AGN activity. In a separate study (Harker et al. 2006) we show that quenching models provide a better match than frosting models to the Balmer line data presented in this Letter and to the growth in the number density of red galaxies from $z \sim 1.4$ to the present day (e.g., Faber et al. 2006).

A few important caveats must be kept in mind. First, our sample is not yet screened on the basis of morphology; this work is in progress (N. Konidaris et al. 2006, in preparation), but analysis of the spectra of a morphologically defined sample of distant early-type galaxies by Treu et al. (2005) yielded similar results. It is also important to keep in mind that we are dealing with a field sample. Previous studies of cluster samples at comparable redshifts tell a different story, with cluster RSGs indicating high z_{form} (e.g., Kelson et al. 2001). Finally, the local SDSS sample used here does not match perfectly the selection criteria adopted for our DEEP2 sample. In particular, unlike our sample, that of Eisenstein et al. has no emission-line cut. Work aimed at producing more adequate local counterparts to our distant DEEP2 sample is currently underway (G. Graves et al. 2006, in preparation).

This project was supported in part by NSF grants AST 00-71198, AST 00-71408, and AST 05-07483. R. P. S. acknowledges financial support from *HST* Treasury Program grant GO-09455.05-A to the University of Virginia. R. P. S. thanks Bob O’Connell and Jim Rose for helpful comments on an early version of the manuscript. The referee is thanked for insightful comments. J. A. N. acknowledges support from NASA through Hubble Fellowship grant HST-HF-01165.01-A awarded by the Space Telescope Science Institute, which is operated by the Association of Universities for Research in Astronomy, Inc., for NASA, under contract NAS5-26555. We thank the Hawaiian people for allowing us to conduct observations from their sacred mountain.

REFERENCES

- Bell, E., et al. 2004, *ApJ*, 608, 752
 Caldwell, N., Rose, J. A., & Concannon, K. D. 2003, *AJ*, 125, 2891
 Daddi, E., et al. 2005, *ApJ*, 626, 680
 Davis, M., et al. 2003, *Proc. SPIE*, 4834, 161
 Eisenstein, D., et al. 2003, *ApJ*, 585, 694
 Faber, S. M., et al. 2003, *Proc. SPIE*, 4841, 1657
 ———. 2006, *ApJ*, submitted (astro-ph/0506044)
 Fisher, D., Fabricant, D., Franx, M., & van Dokkum, P. 1998, *ApJ*, 498, 195
 Gebhardt, K., et al. 2003, *ApJ*, 597, 239
 González, J. J. 1993, Ph.D. thesis, Univ. California, Santa Cruz
 Harker, J. J., Schiavon, R. P., Weiner, B. J., & Faber, S. M. 2006, *ApJ*, 647, L103
 Kelson, D. D., Illingworth, G. D., Franx, M., & van Dokkum, P. G. 2001, *ApJ*, 552, L17
 Kuntschner, H. 2000, *MNRAS*, 315, 184
 Le Borgne, D., et al. 2006, *ApJ*, 642, 48
 Longhetti, M., et al. 2005, *MNRAS*, 361, 897
 MacArthur, L. A. 2005, *ApJ*, 623, 795
 Phillips, M. M., Jenkins, C. R., Dopita, M. A., Sadler, A. M., & Binette, L. 1986, *AJ*, 91, 1062
 Rampazzo, R., Annibali, F., Bressan, A., Longhetti, M., Padoan, F., & Roldighiero, G. 2005, *A&A*, 433, 497
 Schiavon, R. P. 2006, *ApJS*, submitted
 Schweizer, F., & Seitzer, P. 1992, *AJ*, 104, 1039
 Spergel, D. N., et al. 2003, *ApJS*, 148, 175
 Thomas, D., Maraston, C., Bender, R., & Mendes de Oliveira, C. 2005, *ApJ*, 621, 673
 Trager, S. C., Faber, S. M., Worthey, G., & González, J. J. 2000, *AJ*, 120, 165
 Treu, T., et al. 2005, *ApJ*, 633, 174
 Weiner, B. J., et al. 2005, *ApJ*, 620, 595
 Willmer, C. N. A., et al. 2006, *ApJ*, 647, 853
 Worthey, G., Faber, S. M., González, J. J., & Burstein, D. 1994, *ApJS*, 94, 687
 Worthey, G., & Ottaviani, D. L. 1997, *ApJS*, 111, 377
 Yan, R., Newman, J. A., Faber, S. M., Konidaris, N., Koo, D., & Davis, M. 2006, *ApJ*, 648, 281

Note added in proof.—Because the young/intermediate age stars present in RSG galaxies have a stronger impact on H δ than on Fe4383, an SSP analysis of blue spectra tends to bias the results toward higher [Fe/H], by roughly 0.2 dex, compared to an analysis based on the redder Lick indices, such as H β and Fe. Therefore, more realistic mean values for [Fe/H] can be obtained by subtracting 0.2 dex from the values inferred from Figure 2*b*. Modeling of this effect will be presented in a forthcoming publication (J. Harker et al. 2006, in preparation).